Mixed Convection Heat Transfer in a Cavity with Rotating Cylinder Under the Influence of Magnetic Field

Ranjit J. Singh and Trushar B. Gohil

Abstract The present study investigates the influence of magnetic field on the heat transfer phenomena of rotating cylinder kept in the center of the square cavity. The numerical code for mixed convective flow with Magnetohydrodynamics is developed on the open-source CFD platform OpenFOAM. The developed solver is capable of simulating steady and unsteady flows on any arbitrary geometry. The center of the cylinder is fixed at the center of the cavity with varying blockage ratio (L/d = 2 and 4). The surface of the cylinder is kept as hot, and the two opposite vertical sides are kept cold, while the top and bottom surface are maintained as thermally insulated. The cylinder is rotated clockwise (ω = 50) and anticlockwise (ω = −50) about its center. The fluid is assumed to be incompressible and electric conducting in nature and the all walls of the cavity is also maintained as electrically insulated. The intensity of magnetic field is varied in terms of Hartmann number (Ha) in the range of Ha = 0 and 100 for the fixed Rayleigh number of $Ra = 10^5$. The flow and thermal field are analyzed through streamlines, isotherm contours for various Ha and ω (angular rotation). Furthermore, pertinent transport quantities as the Nusselt number is also determined to analyze the influence of magnetic field and angular rotation of the cylinder on the heat transfer. It is observed that the heat transfer and fluid flow behavior is significantly affected by the magnetic field and rotation of the cylinder.

Keywords OpenFOAM · MHD · Mixed convection · Rotating cylinder

Nomenclature

U	Velocity of fluid (m s^{-1})
p	Pressure (N m^{-2})
T	Temperature (K)
T_{ref}	Ambient temperature (K)

R. J. Singh · T. B. Gohil (✉)
Department of Mechanical Engineering, Visvesvaraya National Institute of Technology, Nagpur 440010, India
e-mail: trushar.gohil@gmail.com

P. Saha et al. (eds.), *Advances in Fluid and Thermal Engineering*,
Lecture Notes in Mechanical Engineering,
https://doi.org/10.1007/978-981-13-6416-7_6

j Electric current density (A m^{-2})
B Applied magnetic field (kg s^{-2} A^{-1})
g Acceleration due to gravity (m s^{-2})
ϕ Electric potential (m^2 kg s^{-3} A^{-1})
L Side length of cube (m)
Gr Grashof number
Ha Hartmann number
Ra Rayleigh number
F Lorentz force ($j \times B$) (N m^{-3})
Pr Prandtl number
Nu Nusselt number
d Diameter of cylinder (m)
ω Angular velocity (rad/s)
x, y Cartesian coordinates (m)

Greek symbols

α Thermal diffusivity (m^2 s^{-1})
β Coefficient of thermal expansion (K^{-1})
ρ Fluid density (kg m^{-3})
σ Fluid electrical conductivity (s^3 A^2 m^{-3} kg^{-1})
μ Dynamic viscosity (kg m^{-1} s^{-1})
ν Kinematic viscosity (m^2 s^{-1})

1 Introduction

Since few decades, the numerical analysis of convectional heat transfer and fluid flow has come to be one of the essential engineering applications in industrial or commercial fields. The active or passive regulation of heat and fluid flow are enormously vital in the designing of nuclear reactors, heat exchanger, cooling of electronic components, etc. It has been observed that the most of the researches are concentrated on the natural convection flow with the existence of bodies bounded within enclosures. Various exploration have dealt with the presence of the object with different thermal circumstances on natural convection within the square domain with either horizontal [1, 2] and vertical [3, 4] temperature difference or heat flux. Asan [5] numerically analyzed the free convection flow in the two-dimensional concentric isothermal square annulus for the Rayleigh number of Ra up to 10^6. The obtained results showed that the Rayleigh number (Ra) and aspect ratio have a substantial effect on the heat transfer and flow fields. Ghaddar [6] presented the numerical outcomes for the heated horizontal cylinder located inside the big rectangular enclosure. It was observed that the thermal and flow

performance be contingent on the heat flux applied to the inner cylinder and got the correlation between the Nusselt number and Rayleigh number. Kim et al. [7] observed the numerical assessment of the natural convection arise by the temperature variation by the heated inner cylinder and the cold outer surface of different *Ra* ranges vary from 10^3 to 10^7.

The size, quantity, and development of convection rolls depend on the location of the cylinder altered in the centerline of the outer domain and the Rayleigh number. Reymond et al. [8] had executed the experimentation on the free convection heat and fluid flow from a couple of vertically attached horizontal cylinders at various Rayleigh numbers and cylinder positioning. It is revealed that the presence of lower cold cylinder does not disturb the heat dissipation and fluid flow for the heated upper cylinder. Conversely, when the top and bottom cylinders are kept hot, then the heat dissipation and fluid flow close to the hot upper cylinder is intensely influenced because the plume emerging from heated lower cylinder intermingles with heated upper cylinder. Kareem et al. [9] numerically inspected the turbulent heat dissipation and fluid flow in the three-dimensional lid-driven enclosure with rotating cylinders. The large eddy simulation (LES) and unsteady Reynolds-averaged Navier–Stokes (URANS) approaches are assumed to analyze the fluid flow and heat transfer; it is shown that LES can predict the structure details of secondary vortices that have strong upshot on heat transfer. Chatterjee et al. [10, 11] considered the heat and fluid flow under the lid-driven square enclosure, and static enclosure for the rotating cylinder positioned at the center of the cavity. It has been perceived that the heat transfer is highly affected by the angular rotation of the cylinder. Park et al. [12] numerically observed the free convection heat and fluid flow in the square domain with static cylinder kept at the different position. The result revealed that the increase in the gap between the center of cylinder to the square cavity and Rayleigh number the heat transfer upsurges.

In this present numerical observation, The MHD-based free convection heat and fluid flow solver are established in the OpenFOAM to carry out the numerical investigation of the fluid flow and heat transfer rate under the impact of the magnetic field. The comparison of streamlines, isotherms, and Nusselt number over the heated cylinder under the influence of magnetic field with the angular rotation of cylinder at $\omega = 50$ (clockwise (CW) and counter-clockwise (CCW) and stationary conditions are reported. The streamlines, isotherms, and the Nusselt number show the significant variation in the presence of magnetic field.

2 Mathematical Formulations and Numerical Scheme

Let us consider the steady buoyancy-driven natural convection flow in the cubic cavity heated from inner cylinder within the square enclosure. The physical transport properties fluid is supposed to be independent of temperature. The working fluid is assumed to be viscous, incompressible, and electrically conducting. The thermal and electrical conductivity of outer wall is expected to be uniform.

Therefore, the governing equation for present numerical analysis can be written as follows:

Continuity equation:

$$\nabla \cdot \vec{U} = 0 \tag{1}$$

Momentum equation with Lorentz force and Boussinesq approximation:

$$\frac{\partial \vec{U}}{\partial t} + (\vec{U} \cdot \nabla)\vec{U} = -\frac{\nabla p}{\rho} + \nu \cdot \nabla^2 \vec{U} + \frac{\vec{j} \times \vec{B}}{\rho} - \beta(T - T_{\text{ref}})\vec{g} \tag{2}$$

Ohm's law current density for fluid:

$$\vec{j} = \sigma(-\nabla\phi + \vec{U} \times \vec{B}) \tag{3}$$

Conservation of charge:

$$\nabla \cdot \vec{j} = 0 \tag{4}$$

Conservation of thermal energy of fluid:

$$\frac{\partial T}{\partial t} + (\vec{U} \cdot \nabla)T = \nabla \cdot (\alpha . \nabla T) \tag{5}$$

The Poison's electric potential equation is completed by correlating the Ohm's law of current density (Eq. 3) and conservation of charge (Eq. 4) is mentioned as follow:

$$\nabla^2 \phi = \nabla \cdot (\vec{U} \times \vec{B}) \tag{6}$$

The three non-dimensional parameters included in this investigation to observe the fluid behavior under the effect of magnetic field are as follows:

$$Ha = BL\sqrt{\frac{\sigma}{\rho \nu}} Ra = \frac{g\beta(T - T_{ref})L^3}{\nu\alpha} = Gr \cdot Pr = {}^{\nu}/_{\alpha}$$

where the *Ha* is the Hartmann number, which is used to estimate the intensity of magnetic field. It is defined as the ratio of Lorentz force to viscous force. The *Ra* is the Rayleigh number, expresses the range of stability of fluid (laminar or unsteady). Grashof number narrates the association between the buoyancy and viscosity of the fluid and the Prandtl number expresses the association between momentum diffusivity and thermal diffusivity. Here, *L* stands for the characteristic length taken as the side length of cube. The present solver computes the Eqs. 1–6 using PIMPLE algorithm. The Boussinesq approximation is included in the solver to get buoyancy effect in the fluid. The Rhie and Chow [13] interpolation scheme is available in the

Table 1 Boundary conditions and non-dimensional parameters

Parameters	Cylinder	Right and left side walls	Top/bottom
U	ω = 0 and 50 (CW and CCW)	No slip	No slip
p	$\partial p/\partial n = 0$		
T	1	0	$\partial T/\partial n = 0$
ϕ	$\partial \phi/\partial n = 0$		
Ra	10^5 (Ha = 0 and 100)		
Pr	0.71		

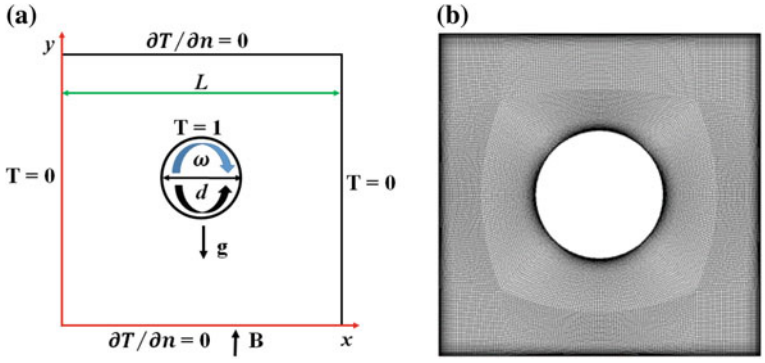

Fig. 1 **a** Schematic view of square enclosure with cylinder and **b** mesh distribution at the plane z = 0.5

solver to compute the Navier–Stokes equation, where velocity is attained from momentum equation and pressure is obtained from continuity equation. Henceforth, the velocity is employed to obtain the electric potential, electric current, and hence Lorentz force. The Lorentz force behaves as source term along with Boussinesq approximation in the momentum equation. The Euler and second-order central difference scheme are used to discretize the time derivate and convection as well as diffusion term, respectively. Table 1 illustrates the boundary condition and non-dimensional parameters utilized in the present study to perform numerical simulations (Fig. 1).

3 Validation and Grid Independence Test

The results produced from the present solver have been validated with the results revealed in the published literature by Chatterjee et al. [14]. The physical boundary condition and geometrical information are retained same as mentioned in the reference [14]. Figure 2a confirmed the velocity profile comparison attained in the vertical y-direction with reference [14]. The grid independence test is performed on

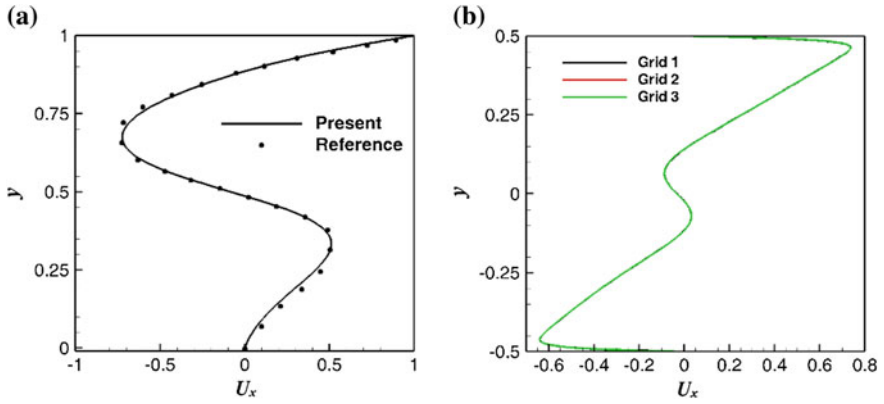

Fig. 2 **a** Comparison of the horizontal velocity along the vertical y-direction at $x = 0.25$, $\omega = 50$ with Ref. [14]. **b** Grid independence

three different grid sizes for $Ra = 10^5$ and $Ha = 100$ and $\omega = 50$ (CW) as follows; grid 1 = 20,000 elements, grid 2 = 30,000 elements, and grid 3 = 40,000 elements. Figure 2b expresses the grid independence comparison and hence the grid 2 can be decided for further computation, as it has enough mesh quality to accommodate all the boundary layer physics.

4 Results and Discussion

The present study is focused to investigate the mutual effect of buoyancy-driven flow with the angular rotation of cylinder in the free convection flow. The Rayleigh number and angular rotation of cylinder for the present analysis is fixed as $Ra = 10^5$; $\omega = 0$ and 50 rad/s (CW and CCW). The intensity of magnetic field is fixed at $Ha = 0$ and 100, which has the substantial outcome on the heat transfer and fluid flow structures. Figure 3 shows the streamlines for the stationary as well as rotating cylinder at $Ha = 0$ and 100 for $L/d = 2$ and 4, expresses the uniform distribution of flow on both sides for $Ha = 0$. As soon as the rotation is given to the cylinder, it has been observed that the flow pattern is shifted in the direction of rotation and the angular rotation of the cylinder results into the uneven distribution of the flow. The magnetic field is applied in the vertical direction against the gravity. The non-uniform distribution of the flow (Fig. 3b, c, h, and i) at an angular rotation of $\omega = 50$ (CW and CCW) brought to the uniform pattern at low intensity of magnetic field ($Ha = 50$) imposed on system as shown in Fig. 3e, f, k, and l. Similarly, Fig. 4 reveals the temperature contours and isotherms pattern at different magnetic field intensity and angular rotation. It has been observed from the isotherms that the plume generated by the ordinary convection flow has dissipation pattern as per the buoyancy force and centrifugal force offered by the rotation of the

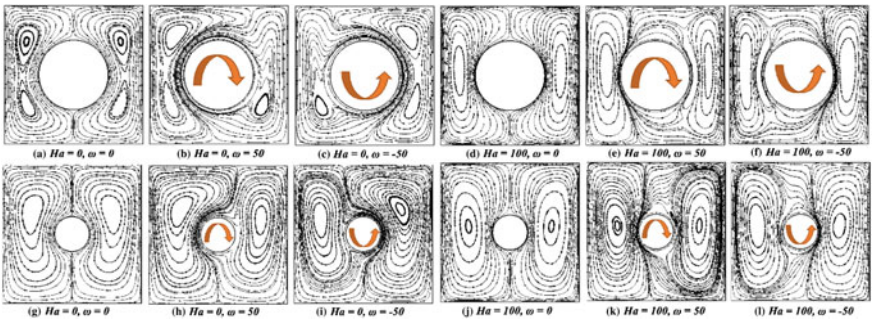

Fig. 3 Streamline variations for L/d = 2 (top) and L/d = 4 (bottom)

cylinder. The application of magnetic field produces the electric current, which further interacts with the magnetic field to produce Lorentz force. The Lorentz force has the direction of flow opposite to the flow of the fluid. Hence, it opposes the flow of fluid in the cavity and hence the plume. Therefore, isotherms are distributed independently of rotation of cylinder as the Lorentz force is balancing the centrifugal force offered by the cylinder. Figure 4e, f, k, and l shows the isotherms which are against the rotation of cylinder and Fig. 5 shows the local Nusselt number variation over the hot cylindrical surface at different Hartmann number and angular rotation. It has been observed from Fig. 5a and b that the peak value of local Nusselt number increases with rotation. In the case of L/d = 4, there is a decrement in the peak local Nusselt number is observed with the application of magnetic field and angular rotation. The centrifugal forces in the domain offered by the angular rotation of smaller cylinder do not overcome the buoyancy forces compared to larger cylinder. Hence, the heat dissipation is constricted by the magnetic field even at the angular rotation of the smaller cylinder. Figure 6a and b shows the variation of horizontal component of velocity (U_x) along the vertical y-direction at the plane x = 0.25. It is understood from Fig. 6a that the larger diameter

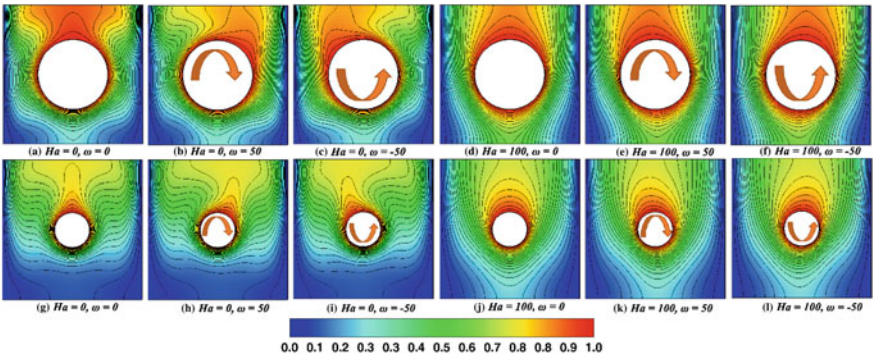

Fig. 4 Temperature Isotherms variation for L/d = 2 (top) and L/d = 4 (bottom)

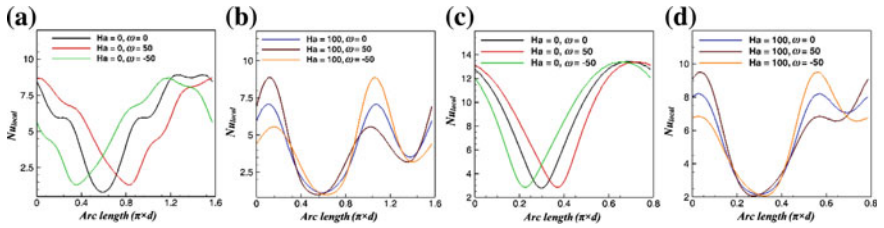

Fig. 5 Local Nusselt number variation over the surface of cylinder for $L/d = 2$ (**a** and **b**) and $L/d = 4$ (**c** and **d**)

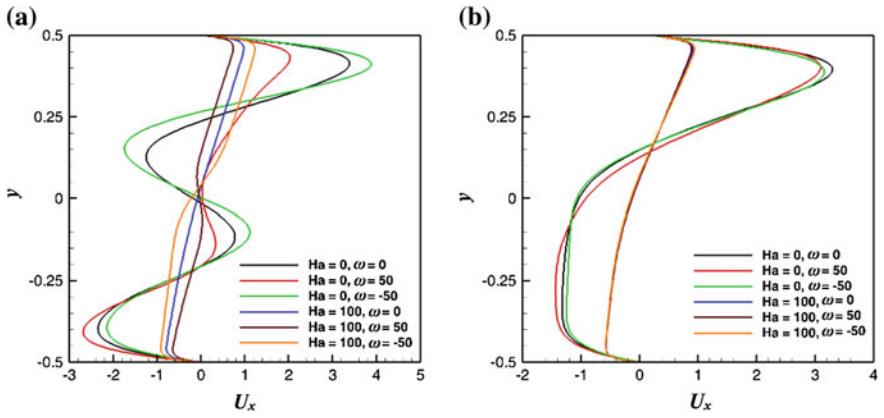

Fig. 6 Comparison of horizontal component pof velocity (U_x) along the vertical y-direction at different Ha and ω at the plane $x = 0.25$, **a** $L/d = 4$ and **b** $L/d = 4$

of the cylinder has a substantial effect on the flow distribution in the domain even at the higher magnetic field. The velocity variation in the case of the smaller cylinder (Fig. 6b) does not have any significant change in the flow behavior even at the angular motion, this is happening because of the high magnetic field opposing the flow motion and low centrifugal force offered by the smaller cylinder.

5 Conclusion

The present examination is focused on the transformation in the flow and heat dissipation structure within a square enclosure with hot rotating cylinder under the impact of magnetic strength. The angular rotation of the cylinder is kept uniform at $\omega = 50$ (CW and CCW) with the variable magnetic field strength of $Ha = 0$ and 100. The Rayleigh number of the system is kept at $Ra = 10^5$ with Prandtl number of $Pr = 0.71$. It is understood from the results when the cylinder is stationary the flow

and heat transfer follow the steady nature, as soon as the cylinder started the angular rotation the shift in the heat transfer and flow pattern begins. This shifting in the flow pattern shows the effect of centrifugal force in the domain. Furthermore, the application of magnetic field assists to bring the shifted nature of the flow structure and Nusselt number in a symmetrical form which can be seen in Figs. 5 and 6. However, the magnetic intensity reduced the heat transfer rate and regulated the flow pattern in the regular sequences, which can be seen in Fig. 4. The Nusselt number at stationary cylinder without magnetic field is higher compared with the system imposed with the magnetic field. This is so because the intensity of the magnetic field ($Ha = 50$) consequently suppresses the flow affecting the drop in the heat transfer. Figure 6 shows the decrease in the peak velocity when the magnetic field of $Ha = 50$ is applied to the system.

Acknowledgements Authors are sincerely gratified to government of India for contributing the financial support through MHRD scholarship to conduct the present numerical investigation.

References

1. Ha MY, Kim IK, Yoon HS, Lee SS (2002) Unsteady fluid flow and temperature fields in a horizontal enclosure with an adiabatic body. Phys Fluids 14:3189–3202
2. Lee JR, Ha MY (2015) A numerical study of natural convection in a horizontal enclosure with a conducting body. Int J Heat Mass Transfer 48:3308–3318
3. Misra D, Sarkar A (1997) Finite element analysis of conjugate natural convection in a square enclosure with a conducting vertical wall. Comput Methods Appl Mech Eng 141:205–219
4. Jami M, Mezrhab A, Bouzidi M, Lallemand P (2007) Lattice Boltzmann method applied to the laminar natural convection in an enclosure with a heat-generating cylinder conducting body. Int J Thermal Sci 46:38–47
5. Asan H (2000) Natural convection in an annulus between two isothermal concentric square ducts. Int Comm Heat Mass Transfer 27:367–376
6. Ghaddar NK (1992) Natural convection heat transfer between a uniformly heated cylindrical element and its rectangular enclosure. Int J Heat Mass Transfer 35:2327–2334
7. Kim BS, Lee DS, Ha MY, Yoon HS (2008) A numerical study of natural convection in a square enclosure with a circular cylinder at different vertical locations. Int J Heat Mass Transfer 51:1888–1906
8. Reymond O, Murray DB, O'Donovan TS (2008) Natural convection heat transfer from two horizontal cylinders. Exp Thermal Fluid Sci 32:1702–1709
9. Kareem AK, Gao S (2017) Mixed convection heat transfer of turbulent flow in a three-dimensional lid-driven cavity with a rotating cylinder. Int J Heat Mass Transf 112:185–200
10. Chatterjee D, Mondal B, Halder P (2014) Hydromagnetic mixed convective transport in a vertical lid-driven cavity including a Heat conducting rotating circular cylinder. Numer Heat Transfer, Part A 65:48–65
11. Chatterjee D, Halder P (2014) MHD mixed convective transport in square Enclosure with two rotating circular cylinders. Numer Heat Transfer Part A 65:802–824
12. Park YG, Yoon HS, Yeong Ha M (2012) Natural convection in square enclosure with hot and cold cylinders at different vertical locations. Int J Heat Mass Transf 55:7911–7925

13. Ferziger JH, Peric M (2002) Computational Methods for Fluid Dynamics, 3rd edn. Springer, Verlag Berlin Heidelberg, pp 247–251
14. Chatterjee D, Gupta SK, Mondal B (2014) Mixed convective transport in a lid-driven cavity containing a nanofluid and a rotating circular cylinder at the center. Int. Commun. Heat Mass Transf 56:71–78